Enhancement of Multi-Walled Carbon Nanotubes Electrical Conductivity using Metal Nanoscale Copper Contacts and its Implications for Carbon Nanotube-Enhanced Copper Conductivity

Chris J. Barnett,[†] James E. McCormack,[‡] Eva M. Deemer,[§] Christopher R. Evans,[¢] Jon E. Evans,[‡] Alvin Orbaek White,[†] Peter R. Dunstan,[¢] Russell R. Chianelli,[§] Richard J. Cobley,[‡] and Andrew R. Barron[†,$,¶*]*

[†] Energy Safety Research Institute, Swansea University, Bay Campus, Swansea SA1 8EN, UK.

[‡] College of Engineering, Swansea University, Bay Campus, Swansea, SA1 8EN, UK

[§] Materials Research and Technology Institute, University of Texas at El Paso, El Paso, Texas TX 79968, USA.

[¢] Department of Physics, College of Science, Swansea University, Singleton Park, Swansea SA2 8PP, UK.

[$] Department of Chemistry and Department of Materials Science and Nanoengineering, Rice University, Houston, Texas 77005, USA.

[¶] Faculty of Engineering, Universiti Teknologi Brunei, Jalan Tungku Link, Gadong, BE1410, Brunei Darussalam

KEYWORDS. Multi-walled carbon nanotube, metal, contact; resistance; Fermi level; copper.

ABSTRACT. Herein we present an experimental/computational approach to probing the interaction between metal contacts and carbon nanotubes (CNTs) with regard creating the most efficient, low resistance, junction. Tungsten probes have been coated with copper or chromium and the efficiency of nano contact transport into multi-walled carbon nanotubes (MWCNTs) has been investigated experimentally, using scanning tunneling spectroscopy (STS) and nanoscale 2-point probe (2PP) I-V measurements, and *in-silico*, employing DFT calculations. Experimental I-V measurements suggest the relative conductivity of the metal-CNT interaction to be Cu > W > Cr. It has been found that copper contacting to MWCNTs results in a high density of state at the Fermi level, which contributes states to the conduction band. It was observed that the density of states also increased when chromium and tungsten probes were contacted to carbon nanotubes; however, in these cases the density of states increase would only contribute in high voltage/high temperature situations. This is demonstrated by an increase in the experimental electrical resistance when compared to the copper probe. These results suggest that in future copper tips should be used when carrying out all intrinsic conduction measurements on CNTs, and they also provide a rational for the ultra-conductivity of Cu-CNT and Cu-graphene composites.

INTRODUCTION

Carbon nanotubes (CNTs) represent an interesting class of material with a diversity of electronic properties. Achiral single walled carbon nanotubes (SWCNTs) are metallic,[1,2] but the rest are either

small or moderate band gap semiconductors,[3] while multi-walled carbon nanotubes (MWCNTs) are usually a zero-gap metals.[4] This diversity offers potential for their use in microelectronic devices.[5,6] In particular, it has been suggested that Cu/low-*k* interconnects are approaching fundamental limits then CNTs are the "most suited for nanometer scale technologies";[7] however, we have recently demonstrated that unless contact effects (including underlying surface contamination) are taken into account, there may be a lower limit that CNT-based devices can be reliably operate.[8]

In our studies on individual MWCNTs and junctions between MWCNTs, we have previously employed tungsten contacts. This is because they are commonly used for scanning probes due to being easily etched to a sharp point and exhibit advantageous electronic properties.[8,9] Other experimental measurements have alternatively employed palladium, titanium or aluminum connections.[10] In order to determine the optimum choice of metal···CNT contact a number of theoretical studies have focused on the choice of metal. These studies aim to investigate tube-electrode transmission to find which metals create prefect or ideal contact conductance. Using first-principles calculations the electron transmission through ideal 2- and 3-terminal junctions between CNTs and metallic (Au or Pd) electrodes has been investigated in a seminal study by Ke.[11] Using first-principles quantum mechanical (QM) density functional and matrix Green's function methods, Goddard and co-workers have reported that the side contact resistance (between a metal electrode and the sidewall of the CNT) followed the trend Pd < Pt < Cu.[12] A similar trend was observed for end contacts (i.e., between a metal electrode and the end of the CNT). In related work, density functional theory (DFT) modeling by Grechnev et al. found that 3d metals on graphene can alter the density of states and therefore alter the conductivity at the interface.[13] It is possible that a similar effect would be observed with metal nano contacts on CNTs. In this regard, an

experimental comparison of the W···CNT contact (as used in our prior studies[8,9]) with a Cr···CNT analog would be of interest.

There have been reports that embedding CNTs in copper increases the conductivity of the copper through the formation of ultra conductive copper (UCC); however, there has been much debate about the exact cause of the effect.[14,15] It has been argued that this effect is caused by better heat distribution due to the CNTs thermal conductivity properties or an increased number of electron pathways or potentially a material enhancement caused by the electronic interactions at the interface.[16,17] If the latter was occurring, it would also explain the reportedly high conductivity of *covetic* materials.[18] Thus, the direct measurement of the Cu···CNT contact is of great interest and practical importance.

Etched tungsten tips have often been used to investigate nanocontacts to nanomaterials and local area electronic structures using STMs and Multi probe systems.[19-21] It is also common for etching to be used when carrying out tip enhanced Raman.[22,23] Often these tips are coated in silver or gold to enhance the plasmon resonance, however, the inactions of the metals at the interface are rarely investigated.

Herein, tungsten STM tips have been coated with chromium and copper and used for I-V and STS measurements on MWCNTs so that the effects of metallic nanocontacts can be investigated. The results are combined with DFT calculations to explain the observed experimental results, including a surprising enhancement of the Cu···CNT system that offers insight into UCC and covetic materials.

METHODS

Materials. MWCNTs were synthesized in table-top horizontal tube reactor at 750 °C with a toluene carbon source and ferrocene as an iron catalyst and cleaned using a microwave to remove

the iron catalyst residue as previously reported.[24,25] 0.15 mm tungsten wire, purchased from Advert, was used to make the tips using KOH flakes (90%) purchased from Honeywell. Copper and chromium were obtained from Kurt J. Lesker Company (Hastings, UK).

Metallization of tungsten tips. Tungsten tips were etched electrochemical in a solution of 2M KOH,[26] loaded into the Omicron LT Nanoprobe, base pressure 10^{-10} mbar, and direct current annealed to 1717 K to remove the native oxide.[27,28] The tips were removed from the vacuum and coated in either copper or chromium. 25 nm of chromium, measured using a crystal monitor, was deposited at room temperature using a Quorum Q150T ES turbomolecular pumped coater (Quorum Technologies Ltd, Laughton, UK) with base pressure 10^{-5} mbar. 25 nm of copper, measured using a crystal monitor, deposited at room temperature using a Pro-Line PVD 75 magnetron sputter deposition tool (Kurt J. Lesker Company, Hastings, UK), base pressure 10^{-7} mbar. The tips were then characterized using a Hitachi S4800 scanning electron microscope (SEM).

Scanning tunneling spectroscopy. Tips were loaded in an Omicron Mirco STM (Scienta Omicron GmbH) and used to carry out STS on highly oriented pyrolytic graphite (HOPG). 100 spectra were collected using each tip with the voltage being swept from -2 V to 2 V. After the STS spectra were taken the tips were brought into contact with the HOPG to ensure that metal coating was mechanically stable. This was achieved by approaching the tip until the current measured reached 333 nA and then approached a further 100 nm. The tips where then characterized again using SEM.

Two-point probe measurements. MWCNTs were loaded into the Nanoprobe and annealed to 500 °C to remove surface contamination and allow consistent contacts to be formed to the tips, as per our previous work.[8] The coated tips were used to carry nanoscale two-point probe on

MWCNTs by approaching using the method describe previously,[29] to ensure pressure on the contact was not an influence. The nanoscale two-point probe (2PP) was carried on a bundle of MWCNTs with one tungsten probe in the same position for all measurements. The second probe was varied in material and brought into contact in five locations on three different nanotubes in a bundle so that the measurements could be directly compared. Our previous work suggests that bundles have little impact on resistance measurements compared to individual nanotubes unless the probes are landed close to a crossing point and that surface contamination can play a significant role.[8,9] It should be noted that as the SEM provides a top down view of the sample and tips, we do not know which part of the tips makes contact with the MWCNTs and there will be uncertainty in the tip position of approximately half the tips radius which may give raise to variations in our measurements. For each measurement the voltage was swept from -0.5 V to 0.5 V to ensure that the direct current annealing was minimized. Five repeat measurements were taking at each location.

DFT calculations. DFT simulations were carried out using generalized gradient approximation (GGA) of Perdew-Burke-Ernzerhof (PBE) that has been used as the exchange correlation potential, which has been used previously to provide a rational band structure for graphene.[30] The spin was set to be unrestricted and formal spin has been used as initial value. The ion core electrons have been replaced by norm-conserving pseudo-potentials and the kinetic energy cut-off value used for plane wave expansions in the chromium and the copper simulations were 400 eV and 600 eV, respectively. It was determined that specifying a cut-off energy of no less than 200 eV provided the optimum balance between computation time and precision, as cut-off energies below this value did not yield significantly varying energies. The total energy changes during the optimization finally converged to less than 1×10^{-5} eV and the forces per atom were reduced to 0.02 eV/Å. The

resulting constraint on spacing of cells in reciprocal space used to generate k-point by a Monkhorst-Pack scheme 2×2×1 was set at 0.07 $Å^{-1}$. These parameters were employed in all calculations. The valence electron configurations for C, Cu, Cr and W are considered as [$2s^2$ $2p^2$], [$3d^{10}$ $4s^1$], [$3d^5$ $4s^1$], and [$5d^4$ $6s^2$], respectively.

RESULTS AND DISCUSSION

SEM. Understanding the interaction between metal contacts and carbon nanotubes is of vital importance if efficient device operation is to be achieved. In order for nanoscale device to be achieve nanoscale contacts must be created and their effects investigated. The coating each tip was imaged using SEM (Figure 1a and b), the tips were then imaged again after being brought into contact with graphite (Figure 1c and d). From Figure 1 it can be seen that the radius of curvature of the tips before contact was ~80 nm. It can also be seen that there is no observable removal of metal after contact with the graphite.

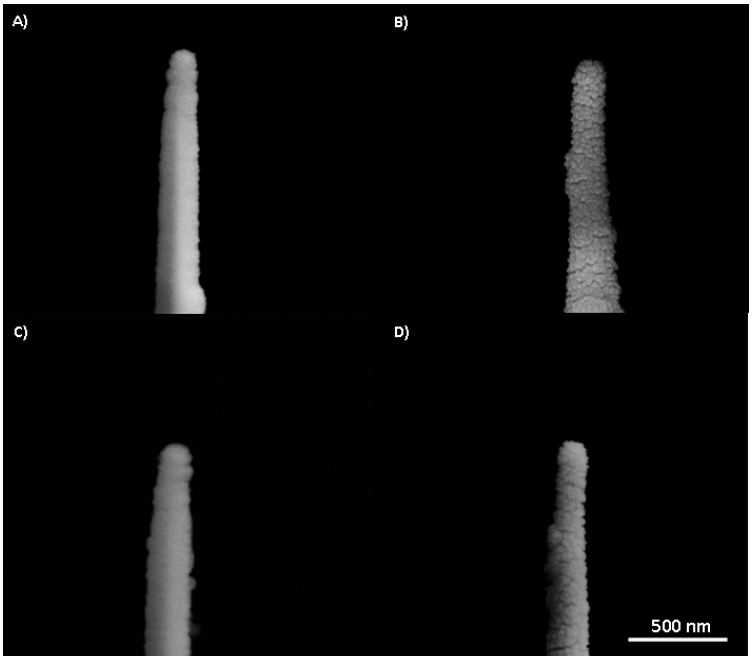

Figure 1. SEM images of tips coated with chromium (a and c) and copper (b and d) before (a and b) and after (c and d) being brought into contact with graphite surfaces.

STS. Scanning tunneling spectroscopy (STS) was carried out on HOPG using the various metal tips to demonstrate that measurements taken are affected by the variance in the work functions of the tip coating metal, i.e., W versus Cr versus Cu. The 100 individual I-V spectra taken with each tip were averaged, and the normalized conductivity (NC) calculated using, Eq. 1, where *c* is a denominator offset constant of 0.02.

$$\frac{dI/dV}{\sqrt{I/V^2+c^2}} = NC \qquad (1)$$

For each metal tip the normalized conductivity was plotted against the applied bias (Figure 2). As may be seen, the current onset of the Cu coated tip is slightly steeper than that of the uncoated W tip, while the Cr coated tip is significantly steeper than both the W tip and Cu coated tip. The slope of each line is an indication of resistance and has a clear dependence on the work function of each metal, i.e., W (4.55 eV) > Cu (4.51 eV) > Cr (4.44 eV). This is due to metals with lower work functions forming lower transport barriers as a result of less band bending when in contact with a n-type semiconductor such as MWCNTs. Thus, each tip behaved as expected for the metal coating, and further confirms that the coated tips behave as per the metal, rather than the underlying tungsten.

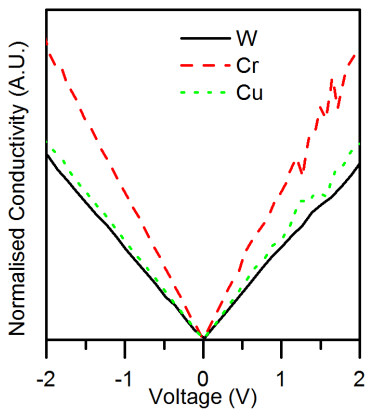

Figure 2. Normalized conductivity as a function of applied bias with a denominator offset constant c = 0.02 on HOPG for probe coatings Cr and Cu, and the uncoated W probe.

Two-point probe conduction measurements. To determine if the same effects observed in the STS translate to contact measurement, nanoscale 2-point probe was carried out on MWCNTs. In each experiment, one tip was placed in set position on MWCNTs with in the network. A second tip was positioned on one of five reproducible locations, within the resolution of the SEM images along the MWCNTs, see Figure S1 in the Electronic Supplementary Material (ESM). In each series the stationary tip was tungsten, while the other is swapped between tungsten, chromium and copper.

The I-V curve is measured five times for each position, for each metal, meaning that a series of I-V curves are obtained for the same positions. The average normalized I-V curve is measured from each position, for each metal. This was done to ensure there was consistency between measurements and no variability due to positions or contact pressure. Figure 3 shows a representative SEM image of a typical position of the tips, along with the associated average normalized I-V curve; the remaining four positions and corresponding I-V are shown in Figure S1 (ESM). The normalized averaged I-V curves are calculated by normalized the IV spectra to the current at 0.5 V then averaged. The normalized I-V curve is shown in Figure 3b to show that there is no change in the contact type, which would alter the shape of the plot, the resistance is calculate for the average current at 0.1 V. As may be seen from Figure 3, each of the normalized I-V curves, associated with the tip positions, are symmetric indicating no difference in contact between the coated tip and the etched tungsten tip.

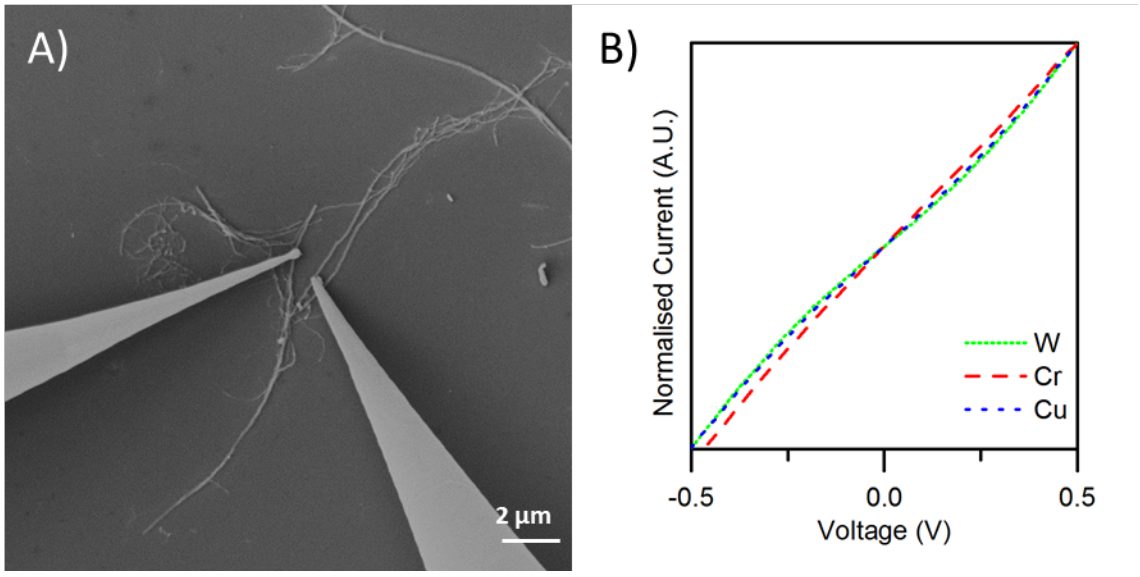

Figure 3. Representative SEM image (a) showing the MWCNT network measured with one of the different tip positions of the floating interchangeable tip (the right tip) as compared to the static W tip (the left tip) and (b) corresponding normalized I-V plot for each metal tip.

As indicated from the STS measurements (see above) and the work function of the metals, the I-V measurements collected with the Cr tip are more ohmic (indicated by a more linear I-V plot) than that collected using the W and Cu tips, irrespective of the tip positions (see Fig. 3). From this observation it would be expected that the resistance measured using the Cr tip would be lower than that using the W and Cu tips; however, this is not the case. The resistance at 0.1 V was calculated for each tip material and position and are shown in Table 1, where it can be seen that the W and Cr coated tip have higher resistance measurements than those taken when the Cu coated tip was used across all five positions. In the cases of Position 1 (Figure 3a) and Position 2 (Figure S1, see ESM) the resistance difference between Cu and the other metal tips is in the region of an order of magnitude. It can also be seen that across all five positions that the resistance measured with the copper coated tip was ~20 kΩ, which is the same as internal resistance of the Nanoprobe therefore we will not observe changes in resistance with probe separation, while the tungsten tip and the

chromium coated tip vary significantly. It should be noted that these values are for W···MWCNT···M (where M = W, Cr, Cu), and thus the changes in conductivity will be amplified by replacement of both tips.

Table 1. Average resistance (kΩ) and uncertainty measured at 0.1 V in each of 5 positions for each metal.

Position	Tip separation (μm)	Average resistance (kΩ)		
		Tungsten	Chromium	Copper
1	5.80	510 ±7.8	140 ±5.3	22 ±0.1
2	5.41	190 ±3.3	290 ±14.1	23 ±0.1
3	4.87	73 ±1.0	90 ±2.1	21 ±0.1
4	4.50	33 ±0.4	28 ±0.8	24 ±0.4
5	5.57	34 ±1.1	24 ±0.2	19 ±0.3

[a] Measured from SEM images assuming shortest pathway between the two tips.

In order to understand the observed differences, we have considered a number of possible explanations: surface contamination, tip separation, individual versus network measurements, different contact areas, variable tip pressure, and metal type. The simplest explanation would be that the variance is caused by surface contamination, which is known to result in, inconsistent, high resistance contacts,[8] but only at small tip separation. If this were a factor, then it would suggest that Cu connects are unaffected by surface contamination given the uniformity of the Cu measurements (Table 1). This explanation would be encouraging for future CNT based devices and suggest that Cu connections would overcome contamination issues. Unfortunately, this is unlikely as the nanotubes were annealed to 500 °C prior to measurements, which is known to remove the surface contamination in prior studies with W tips.[8]

We have reported that for CNT fibers voltage sweeps can be used to clean the fibers[8] and as such it is possible that the measurement using one tip cleans the MWCNT under the tip position such that the subsequent measurements are made with a "cleaned" contact. Given that it was found that a sweep voltage of at least 3 V was required to significantly improve the resistance,[8] and in the present study the voltage sweep was limited to +1 V to -1 V it is highly unlikely this would be a factor. In addition, the measurements on each position were made in the order W, Cu, and Cr tips, thus, if this was a factor the Cr would be expected to be the best and have the most consistent measurements, which is not observed.

We have previously shown that, for tungsten tips, the measured resistance along an individual MWCNT is dependent on the tip separation, and even when cleaned there is a higher resistance for tips closer than 1 μm, due to overlapping depletion zones either side of each the tips.[8] The shortest tip-tip distance in the present study along the network of MWCNTs is ~4 μm (Table 1), thus, the distance is over this critical distance. In addition, the resistance as a function of distance is essentially constant for the Cu tip, while W and Cr show variation (Figure S1, see ESM).

Given the measurements are made on a network of MWCNTs it is possible that the differences in resistance are due to conduction through an individual MWCNT (Position 5) versus network measurements (Positions 1-4). Based upon labeling of the MWCNTs in the network shown in Figure 3a, there are two groups of measurements that involve a junction: W···CNT_A···CNT_B···M and W···CNT_A···CNT_C···M, where M is W, Cr and Cu. Each potential connection is given the designation $M_{A\text{-}B}$ and $M_{A\text{-}C}$, respectively. Positions 1 and 4 are associated with $M_{A\text{-}B}$, while Positions 2 and 3 are associated with $M_{A\text{-}C}$. Consideration of the resistance as a function of distance for each CNT···CNT junction (i.e., separating the resistance from differences in pathway) the values (Table 1) are more consistent with general expectations. From Table 1 (and Figure S1 in the ESM) it is

possible to determine that the resistance increases with tip separation, for each network junction, for W and Cr; however, the values for Cu are independent of both distance and junction. This result would suggest that if the overall resistance in a network is dependent on variability in CNT···CNT junction, then the use of Cu connections would limit such variability: again, suggesting that Cu would be a preferred solution. It is also possible that different metals alter the contact type, however, the STS results (see above) suggest that if this were the case, the Cr tip would have the lowest resistance: the opposite of the experimental data. Also, the normalized I-V show the contact type is not affect by the material used to coat the tips.

The observed resistance trends (Table 1) could be a result of contact areas,[12] due to the thicker chromium (radius 90 nm) and copper tips (radius 63 nm). If this were true then the values for Cr would also having a lower resistance than the W (radius 40 nm), which is not the case for all Positions (Table 1). In addition, the method used to approach the tip reduces the chances of tip pressure altering the measurements.[29] We can, therefore, eliminate contact area and pressure as a contributing factor to these measurements. In 3 positions, the measure resistance when using the tungsten probe is higher than that using the chromium coated probe which agrees with theory of tip area above. In the 2 positions where the chromium tip measured higher in resistance could be attributed to landing on contamination or section of damaged nanotube, as the uncertainty also show to be higher.

Based upon the proceeding, a Cu tip shows consistently lower electrical resistance measurements in comparison to W or Cr tips. In part, this is counter to expectations based upon the work function of the metal, but it is possible that this lowering in the electrical resistance for Cu tip is due to it being less susceptible to surface contamination of the CNT and the presence of CNT···CNT junctions. From the experimental results, it is unclear what the reasons for this advantage would

be; however, both would represent significant practical advantages when fabricating CNT-based devices. Irrespective of these issues, it is clear that in all cases the use of a Cu tip results in a lower overall resistance suggesting the Cu···CNT interaction is of importance.

DFT Calculations. To understand what is happening at the tip···CNT interface that results in the copper coated tip measuring lower resistance at 0.1 V a density functional theory (DFT) and plane-wave pseudopotential model has been created using CASTEP code with a graphene sheet used to represent the surface of the MWCNT due to the difficulty for preforming computational analysis using MWCNTs using first principle calculations.[31-39]

The density of states for each metal-on-CNT system is shown in Figure 4. It can be seen that that when Cu in contacted to the carbon (Fig. 4a), new states are created around the Fermi energy due to the interaction between Cu 3d and C 2p electrons (Figure S2a and b, see ESM), which facilitates electron transport. It can also be seen that there is a large increase in the number of states around -2 eV that will result in increased conduction at elevated energies such as when heated. This is consistent with the increased conductivity of Cu-CNT hybrid materials at elevated temperatures.[17]

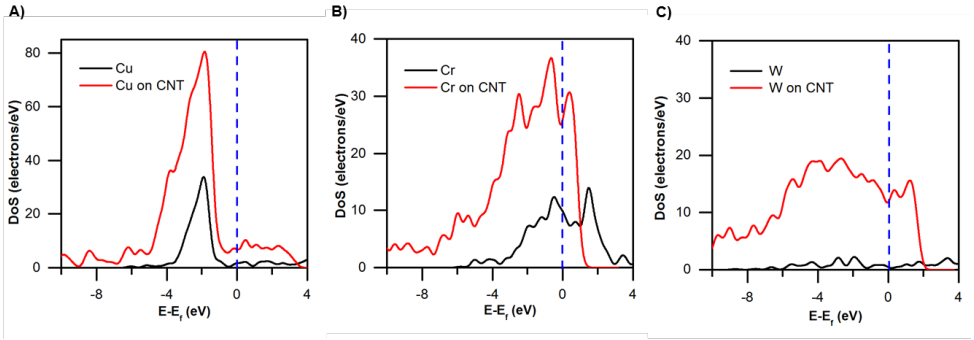

Figure 4 DOS plots a) for copper cell (black) and for the simulated copper on carbon nanotube (red), b) for chromium cell (black) and for the simulated chromium on carbon nanotube (red) and c) for tungsten cell (black) and for the simulated tungsten on carbon nanotube (red) blue line indicates the Fermi level.

For chromium, there is a strong hybridization between C 2s and 2p electrons and Cr 4d electrons around -5 eV (Figure S2, see ESM) and appears to slightly shift away from the Fermi energy due to the combination of its 3d orbital overlap with carbon s and p orbitals. While the increasing number of states could serve as an advantage in higher voltage transport applications, there is not an appreciable change at the Fermi energy. Tungsten should show similar results to chromium being in the same group in the periodic table, however the ground electronic state of tungsten has an important difference; in that instead of having an electron from the s orbital hybridized to form a half-filled d shell, tungsten has filled a 6s shell.

Copper, however, shows a clear advantage in hybridized Cu d orbitals at the Fermi energy while the unoccupied p orbital contributes states to the conduction band in the electronic band structure. These findings are supported by previous theoretical investigations performed on a contact configuration simulated by a metallic single wall carbon nanotube and linear copper chain.[34] Authors of the study found that Cu atoms positioned in front of the CNT's carbon atom significantly influence the electronic properties of the entire hybrid system. Moreover, the hybrid system was shown to induce a sizeable charge transfer from the Cu 4s and 3d states to the C atom of the tube. Therefore, a higher number of electronic states are made available, thus increasing the systems total DOS compared pristine Cu or C alone. Studies performed on Cu nanoclusters on zig-zag graphene nanoribbons have also revealed the same hybridization of p and d orbitals between C and Cu in DOS simulations.[39-40] An additional study on the impact these effects have on the transport of the nanoribbons determined that copper can alter the current-voltage characteristics and create a negative differential resistance.[41]

When comparing the electronic band structure, shown in Figure S3 (in the ESM), of the three simulations, we discover that in all cases where sp^2 carbon is at the surface of these transition

metals, bands shift states to the valence band and carriers heavily occupy states below the Fermi energy. Chromium shows the most extreme Fermi "pinching" in these comparisons which can be analogous to the Fermi band pinning effect between metal-semiconductor junctions that play a large role in device performance and very pronounced in nano devices. Chromium shows the most extreme Fermi "pinching" in these comparisons which can be analogous to the Fermi band pinning effect between metal-semiconductor junctions that play a large role in device performance and very pronounced in nano devices. Fermi pinning is a well-known phenomenon that occurs at the interface of a metal/semiconductor junction, in which the DOS is finite, where the bandgap in a semiconductor is locked to the Fermi level.

In chromium, the electronic band structure is constricted in the conduction bands above the Fermi level while filling the valence bands. These constricted bands decrease mobility as electrons in metals moving freely between the conduction band and valence band along these energy bands require empty bands to scatter into. We evidence this shift with the partial DOS and show unfilled p orbital are largely contributing to carrier states at the Fermi energy. These simulations describing transition metal-C interfaces offer insight into the nature of intrinsic contact resistance in nanocarbon based devices, which is of enormous consequence when considering the optimizations at such small thresholds.

CONCLUSIONS

Coated STM probes have been used to investigate the transport mechanism on copper, tungsten and chromium nanocontact to MWCNTs. STS results suggest that chromium coated tips should result in lower resistance measurement due to the lower work function; however, nano scale 2PP I-V measurements showed that copper coated tips result in significantly lower resistance measurements. DFT simulations suggest that this was a result of increased density of state close

to the Fermi level when copper is in contact with carbon due to interaction between Cu 3d and C 2p electrons, resulting in increased transport through the junction. Although the chromium contacts also showed an increase in the number density of states, the density of states was shift towards a lower energy and therefore would only facilitate increased transport at high voltages.

These results suggest that in-order to measure the intrinsic resistance of carbon nanotubes with probe-based technique then copper tips should be used to maximize the current flow at the interface between tip and tube. Our work also offers an explanation as to why copper embedded with carbon nanotubes shows ultra-conductivity and the observations of other groups[41,42]. The work suggests that copper in contact with CNTs will have increased density of states at the Fermi, which facilitates electron transfer and therefore lower resistance. The results also show higher number of states above the Fermi level, which will cause increased transport at high energies such as when heated about room temperature. Finally, these experimentally and theatrically illustrated fundamental principles related to ultra-conductive copper produced from the combination of Cu and CNTs. If it is the interface between the Cu and CNT that facilitates the increased conductivity of UCC over copper, then the challenge to maximize the dispersion of CNTs into the Cu matrix should be the focus of future research.

ASSOCIATED CONTENT

Supporting Information. The Supporting Information is available free of charge at https://pubs.acs.org/doi/XXXXXXX. SEM images of the tip positions and corresponding normalized I-V graphs; diagrams of the partial density of states; electronic band structures for M-CNT.

AUTHOR INFORMATION

Corresponding Author

* Authors to whom correspondence should be addressed: a.r.barron@swansea.ac.uk or chianell@utep.edu

Author Contributions

The manuscript was written through contributions of all authors. All authors have given approval to the final version of the manuscript.

Notes

The authors declare no competing financial interest.

ACKNOWLEDGMENT

Financial support was provided by the Office of Naval Research (N00014-15-2717), the Welsh Government Sêr Cymru Programme through Sêr Cymru II Welsh Fellowships (and A.O.W.) part funded by the European Regional Development Fund (ERDF), the Sêr Cymru Chair for Low Carbon Energy and Environment (A.R.B), the Reducing Industrial Carbon Emissions (RICE) operations funded by the Welsh European Funding Office (WEFO) through the Welsh Government, and the Robert A. Welch Foundation (C-0002).

REFERENCES

(1) Wei, B. Q.; Vajtai, R.; Ajayan, P. M. Reliability and current carrying capacity of carbon nanotubes. *Appl. Phys. Lett.* **2001**, *79*, 1172–1174.

(2) Yao, Z.; Kane, C. L.; Dekker, C. High-field electrical transport in single-wall carbon nanotubes. *Phys. Rev. Lett.* **2000**, *84*, 2941–2944.

(3) Stobbe, S.; Lindelof, P. E.; Nygård, J. Integration of carbon nanotubes with semiconductor technology: fabrication of hybrid devices by III–V molecular beam epitaxy, *Semicond. Sci. Tech.* **2006**, *21*, S10.

(4) *Das, S.* A review on carbon nano-tubes - a new era of nanotechnology, *Int. J. Emerging Technol. Adv. Eng.* **2013***, 3*, 774-781.

(5) Dayen, J. F.; Wade, T. L.; Konczykowski, M.; Wegrowe, J. E.; Hoffer, X. Conductance in multiwall carbon nanotubes and semiconductor nanowires, *Phys. Rev. B* **2005**, *72*, 073402.

(6) Sun, D. M.; Liu, C.; Ren, W. C.; Cheng, H. M. A review of carbon nanotube and graphene based flexible thin film transistors, *Small* **2013**, *9*, 1188-1205.

(7) Chaudhry, A. Interconnects for nanoscale MOSFET technology: a review, *J. Semicond.* **2013**, *34*, 066001.

(8) Barnett, C. J.; Gowenlock, C.; Welsby, K.; Orbaek White, A.; Barron, A. R. Spatial and contamination dependent electrical properties of carbon nanotubes. *Nano Lett.* **2017**, *18*, 695-700.

(9) Barnett, C. J.; Evans, C.; McCormack, J. E.; Gowenlock, C. E.; Dunstan, P.; Orbaek White, A.; Barron, A. R. Experimental measurement of angular and overlap dependence of conduction between carbon nanotubes of identical chirality and diameter, *Nano Lett.* **2019**, *19*, 4861-4865.

(10) Chen, Z.; Appenzeller, J.; Knoch, J.; Lin, Y.; Avouris, P. The role of metal-nanotube contact in the performance of carbon nanotube field-effect transistors, *Nano Lett.* **2005**, *5*, 1497-1502.

(11) Ke, S.; Yang, W.; Baranger, H. U. Nanotube-metal junctions: 2- and 3-terminal electrical transport, *J. Chem. Phys.* **2006**, *124*, 181102.

(12) Matsuda, Y.; Deng, W.-Q.; Goddard, III, W. A. Contact resistance for "end-contacted" metal–graphene and metal–nanotube interfaces from quantum mechanics, *J. Phys. Chem. C* **2010**, *11*, 17845-17850.

(13) Grechnev, G.E.; Lyogenkaya, A.A.; Kolesnichenko, Y.A.; Prylutskyy, Y.I.; Hayn, R. Electronic structure and magnetic properties of graphite intercalated with 3d-metals. *Low Temp. Phys.* **2014**, *40*, 450-453.

(14) Hjortstam, O.; Isberg, P.; Söderholm, S.; Dai, H. Can we achieve ultra-low resistivity in carbon nanotube-based metal composites? *Appl. Phys. A-Mater* **2004**, *78*, 1175-1179.

(15) Banno, N.; Takeuchi, T. Enhancement of electrical conductivity of copper/carbon-nanotube composite wire. *J Jpn. I. Met.* **2009**, 73, 651-658.

(16) Bao, K. D.; Lu, H.; Grimvall, G. Transverse conductivity in non-ideal fiber composite geometries. *Int. J. Heat Mass Transf.* **1993**, *36*, 4033-4038.

(17) Subramaniam, C.; Yamada, T.; Kobashi, K.; Sekiguchi, A.; Futaba, D. N.; Yumura, M.; Hata, K. One hundred fold increase in current carrying capacity in a carbon nanotube–copper composite. *Nat. Commun.* **2013**, *4*, 2202.

(18) Bakir, M.; Jasiuk, I. Novel metal-carbon nanomaterials: a review on covetics, *Adv. Mater. Lett.* **2017**, *8*, 884-890.

(19) Ekvall, I.; Wahlstrom, E.; Claesson, D.; Olin, H.; Olsson, E. Preparation and characterization of electrochemically etched W tips for STM, *Meas. Sci. Technol.* **1999**, *10*, 11-18.

(20) Muller, A. D.; Muller, F.; Hietschold, M.; Demming, F.; Jersch, J.; Dickmann, K. Characterization of electrochemically etched tungsten tips for scanning tunneling microscopy, *Rev. Sci. Instrum.* **1999**, *70*, 3970-3972.

(21) Ju, B.-F.; Chen, Y.-L.; Ge, Y. The art of electrochemical etching for preparing tungsten probes with controllable tip profile and characteristic parameters, *Rev. Sci. Instrum.* **2011**, 82, 013707.

(22) Meng, L.; Huang, T.; Wang, X.; Chen, S.; Yang, Z.; Ren, B. Gold-coated AFM tips for tip-enhanced Raman spectroscopy: theoretical calculation and experimental demonstration, *Opt. Express* **2015**, *23*, 13804-13813.

(23) Yeo, B.-S.; Zhang, W.; Vannier, C.; Zenobi, R. Enhancement of Raman signals with silver-coated tips. *Appl. Spectrosc.* **2006**, *60*, 1142-1147.

(24) Orbaek, A. W.; Aggarwal, N.; Barron, A. R. The development of a 'process map' for the growth of carbon nanomaterials from ferrocene by injection CVD. *J. Mater. Chem. A* **2013**, *1*, 14122–14132.

(25) Gomez, V.; Irusta, S.; Adams, W. W.; Hauge, R. H.; Dunnill, C. W.; Barron, A. R. Enhanced carbon nanotubes purification by physic-chemical treatment with microwave and Cl_2. *RSC Adv.* **2016**, *6*, 11895-11902.

(26) Ibe, J. P.; Bey, P. P.; Brandow, S. L.; Brizzolara, R. A.; Burnham, N. A.; Dilella, D. P.; Lee, K. P.; Marrian, C. R. K.; Colton, R. J. On the electrochemical etching of tips for scanning tunneling microscopy, *J. Vac. Sci. Technol. A* **1990**, *8*, 3570-3575.

(27) Cobley, R. J.; Brown, R. A.; Barnett, C. J.; Maffeis, T. G. G.; Penny, M. W. Quantitative analysis of annealed scanning probe tips using energy dispersive X-ray spectroscopy, *Appl. Phys. Lett.* **2013**, *102*, 023111.

(28) Barnett, C. J.; Kryvchenkova, O.; Wilson, L. S. J.; Maffeis, T. G. G.; Kalna, K.; Cobley, R. J. The role of probe oxide in local surface conductivity measurements, *J. Appl. Phys.* **2015**, *117*, 174306.

(29) Smith, N. A.; Lord, A. M.; Evans, J. E.; Barnett, C. J.; Cobley, R. J.; Wilks, S. P. Forming reproducible non-lithographic nanocontacts to assess the effect of contact compressive strain in nanomaterials. *Semicond. Sci. Technol.* **2015**, 30, 065011.

(30) Zhou, J.; Wang, Q.; Sun, Q.; Chen, X. S.; Kawazoe, Y.; Jena, P. Ferromagnetism in semihydrogenated graphene sheet. *Nano Lett.* **2009**, *9*, 3867-3870.

(31) Nardelli, M. B.; Fattebert, J. L.; Bernholc, J. O(N) real-space method for ab initio quantum transport calculations: application to carbon nanotube--metal contacts, *Phys. Rev. B* **2001**, *64*, 245423.

(32) Yang, C.-K.; Zhao, J.; Lu, J.P. Binding energies and electronic structures of adsorbed titanium chains on carbon nanotubes, *Phys. Rev. B* **2002**, *66*, 041403.

(33) Chi, D. H.; Cuong, N. T.; Tuan, N. A.; Kim, Y.-T.; Bao, H. T.; Mitani, T.; Ozaki, T.; Nagao, H. Electronic structures of Pt clusters adsorbed on (5,5) single wall carbon nanotube. *Chem. Phys. Lett.* **2006**, *432*, 213-217.

(34) Kong, K.; Han, S.; Ihm, J. Development of an energy barrier at the metal-chain--metallic-carbon-nanotube nanocontact. *Phys. Rev. B* **1999**, *60*, 6074-6079.

(35) Yuan, S.; Wang, X.; Li, P.; Wang, C.; Yuan, S. Structural, wetting, and electronic properties of metal clusters adsorbed on carbon nanotubes, *J. Appl. Phys.* **2008**, *104*, 013509.

(36) Fagan, S. B.; Mota, R.; Antônio, J. R. d. S.; Fazzio, A. An ab initio study of manganese atoms and wires interacting with carbon nanotubes. *J. Phys. Condens. Matter.* **2004**, *16*, 3647.

(37) Fagan, S. B.; Fazzio, A.; Mota, R. Titanium monomers and wires adsorbed on carbon nanotubes: a first principles study. *Nanotechnol.* **2006**, *17*, 1154.

(38) Durgun, E.; Dag, S.; Bagci, V. M. K.; Gülseren, O.; Yildirim, T.; Ciraci, S. Systematic study of adsorption of single atoms on a carbon nanotube. *Phys. Rev. B* **2003**, *67*, 201401.

(39) Berahman, M.; Sheikhi, M. H.; Zarifkar, A.; Nadgaran, H. Structural and electronic properties of zigzag graphene nanoribbon decorated with copper cluster. *J. Comput. Electron.* **2015**, *14*, 270-279.

(40) Berahman, M.; Sheikhi, M. H. Transport properties of zigzag graphene nanoribbon decorated with copper clusters. *J. Appl. Phys.* **2014**, *116*, 093701.

(41) McIntyre, D. J.; Hirschmand, R. K.; Puchades, I.; Landi, B. J. Enhanced copper-carbon nanotube hybrid conductors with titanium adhesion layer. *J Mater. Sci.* **2020**, *55*, 6610-6622.

(42) Sundaram, R.; Yamada, T.; Hata, K.; Sekiguchi, A. Elecxtrical performance of lightweight CNT-Cu composite wires impacted by surface and internal Cu spatial distribution. *Sci. Rep.* **2017**, *7*, 9267.

TOC GRAPHIC